Available online at www.sciencedirect.com

SCIENCE DIRECT®

ELSEVIER

Journal of Solid State Chemistry 177 (2004) 3263–3269

JOURNAL OF SOLID STATE CHEMISTRY

http://elsevier.com/locate/jssc

A novel two-dimensional β-octamolybdate supported alkaline-earth metal complex: $[Ba(DMF)_2(H_2O)]_2[Mo_8O_{26}] \cdot 2DMF$

Chao Qin, Xinlong Wang, Yanfei Qi, Enbo Wang,* Changwen Hu, and Lin Xu

Institute of Polyoxometalate Chemistry, Department of Chemistry, Northeast Normal University, Changchun City, Jilin Province 130024, PR China

Received 15 January 2004; received in revised form 6 May 2004; accepted 21 May 2004

Abstract

A novel β-octamolybdate supported complex $[Ba(DMF)_2(H_2O)]_2[Mo_8O_{26}] \cdot 2DMF$ (**1**) was synthesized by the direct modification to the surface of octamolybdate molecular cluster. Its structure was determined by elemental analysis, TG analysis, IR spectrum, and the single-crystal X-ray diffraction. The title compound crystallizes in triclinic system, space group $P\bar{1}$, $a = 9.984(2)$ Å, $b = 11.117(2)$ Å, $c = 12.681(3)$ Å, $\alpha = 115.86(3)^\circ$, $\beta = 97.66(3)^\circ$, $\gamma = 98.11(3)^\circ$, $V = 1223.5(4)$ Å^3, $Z = 2$, $\lambda(\mathrm{Mo}K\alpha) = 0.71073$ Å, ($R(F) = 0.0386$ for 5535 reflections). Data were collected on a Rigaku R-AXIS RAPID IP diffractometer at 293 K in the range of $2.04 < \theta < 27.47^\circ$. Compound **1** exhibits a novel two-dimensional (2D) layered framework in which all β-$[Mo_8O_{26}]^{4-}$ subunits are connected together through Ba–O–Ba–O–Mo and Ba–O–Mo bridges. Furthermore, these 2D layers are extended into 3D supramolecular network containing parallelogram channels via hydrogen-bonding interactions.

Keywords: Octamolybdate; Barium; Polyoxometalate; Channel; Two-dimensional framework; Crystal structure

1. Introduction

The rapid progress of exploring inorganic solid state materials is driven by the interest of their applications in catalysis, ion exchange, sorption and molecular electronics [1–6]. Polyoxometalates (POM), as an important family of metal oxides, have been receiving considerable attention in solid state materials chemistry, owing to their diverse topological properties and great potential applications in catalysis, photochemistry, electrochromism, medicine, and magnetism [7–9].

So far, one of the synthetic strategies in the field of polyoxometalatic chemistry is to find suitable subunits and then link them up into one-, two-, even three-dimensional (1, 2, even 3D) extended networks, either through direct condensation to form oxo-bridged arrays of cluster or through transition metal coordination compounds acting as inorganic bridging ligands [10]. Using this method, many octamolybdate supported complexes have been reported, e.g. discrete cluster $[\{Cu(2,2'\text{-bpy})\}_2Mo_8O_{26}]$ [11] and $[\{M(phen)_2\}_2(Mo_8O_{26})](M = Ni\,or\,Co)$ [12]; 1D chain $[Ni_2(2,2'\text{-bpy})_4Mo_8O_{26}]$ [13]; 2D layer $[\{Cu(en)_2\}_2Mo_8O_{26}]$ [14], $[\{Ni(4,4'\text{-bpy})_2(H_2O)_2\}_2Mo_8O_{26}]$ [15], and $[\{Cu(pyrd)\}_4Mo_8O_{26}]$ [16], which are all synthesized by hydrothermal methods, MoO_3 or Na_2MoO_4 being initial materials. In contrast, realizing such molecular assemblies by means of the direct modification to the surface of octamolybdate molecular cluster remains a great challenge. To the best of our knowledge, to date, applying the direct route to the preparation of octamolybdate supported compounds with infinitely extended structure has never been reported except two discrete β-octamolybdate supported rare earth metal clustered complexes $[NH_4]_2[\{Gd(DMF)_7\}_2(\beta\text{-}Mo_8O_{26})][\beta\text{-}Mo_8O_{26}]$ and $[NH_4][La(DMF)_7(\beta\text{-}Mo_8O_{26})]$ [17].

Herein, we report the synthesis and single-crystal X-ray analysis of a novel 2D β-octamolybdate supported complex, $[Ba(DMF)_2(H_2O)]_2[Mo_8O_{26}] \cdot 2DMF$ (**1**). It is also the first time that alkaline-earth metal is incorporated into the isopolyoxomolybdates. Moreover, the successful preparation of the compound may contribute to acquiring some information on the optical properties

---

*Corresponding author. Fax: +864315684009.
E-mail address: wangenbo@public.cc.jl.cn (E. Wang).

0022-4596/$ - see front matter © 2004 Elsevier Inc. All rights reserved.
doi:10.1016/j.jssc.2004.05.044

of such kinds of complexes, since polyoxometalate anion are good electron acceptors, while DMF molecule is electron-rich donor, thus the interaction between them would generally lead to electron transfer.

2. Experimental section

2.1. General procedures

All organic solvents and materials used for the synthesis were of regent grade and were used without purification. $[Bu_4N]_4[Mo_8O_{26}]$ was prepared according to the literature method [18]. Element analyses (C, H, N) were performed on a Perkin–Elmer 2400 CHN elemental analyzer. The contents of Mo and Ba were determined by a Leaman inductively coupled plasma (ICP) spectrameter. FTIR spectrum was recorded in the range 400–4000 cm^{-1} on an Alpha Centaurt FTIR spectrophotometer using a KBr pellet. TG analysis was performed on a Perkin–Elmer TGA7 instrument in flowing N_2 with a heating rate of 10°C min^{-1}.

2.2. Synthesis of compound **1**

Five milliliter aqueous solution of $BaCl_2$ (0.5 mmol, 0.1041 g) was added dropwise to a stirred 8 mL DMF solution of $[Bu_4N]_4[Mo_8O_{26}]$, the resulting colorless solution was adjusted to pH ~3.5 with glacial acetic acid, and then was heated at 80°C for half an hour. After the solution had cooled to room temperature, a small amount of white precipitate was filtered off, and the filtrate was allowed to evaporate at room temperature for 2 weeks. Colorless block crystals were collected on a medium porosity sintered glass filter, washed with cold water, and dried in the air (yield: 64% based on Mo). Calc. for $C_9H_{23}BaMo_4N_3O_{17}$ ($M = 966.40$): C, 11.18%; H, 2.40%; N, 4.35%; Mo, 39.71%; Ba, 14.21%. Found: C, 11.3%; H, 2.1%; N, 4.2%; Mo, 39.5%; Ba, 14.3%. FT/IR data (cm^{-1}): 1678(s), 1654(s), 1636(w), 1497(m), 1436(m), 1415(w), 1392(s), 1252(m), 1106(s), 1062(w), 938(s), 912(s), 837(s), 732(w), 694(m), 665(w), 562(m), 526(m).

2.3. X-ray crystallography

The structure of $[Ba(DMF)_2(H_2O)]_2[Mo_8O_{26}] \cdot 2DMF$ was determined by single-crystal X-ray diffraction. Crystallographic data are as follows: $C_9H_{23}BaMo_4N_3O_{17}$, triclinic, $P\bar{1}$, $a = 9.984(2)$ Å, $b = 11.117(2)$ Å, $c = 12.681(3)$ Å, $\alpha = 115.86(3)°$, $\beta = 97.66(3)°$, $\gamma = 98.11(3)°$, $V = 1223.5(4)$ Å^3, $Z = 2$, $D_{cal} = 2.623$ mg/m^3, $\lambda(MoK\alpha) = 0.71073$ Å. A colorless single crystal of the title compound ($0.361 \times 0.335 \times 0.283$ mm^3) was mounted on a glass fiber. Data were collected on a Rigaku R-AXIS RAPID IP diffractometer at room temperature. Empirical absorption correction was applied. The structure was solved by the direct method and refined by the full-matrix least-squares method on F^2 using the SHELXTL crystallographic software package [19]. Anisotropic thermal parameters were used to refine all non-hydrogen atoms. A total of the 8833 (5535 unique, $R_{int} = 0.0424$) reflections were measured. Structure solution and refinement based on 5535 independent reflections with $I > 2\sigma(I)$ and 308 parameters gave $R_1(wR_2) = 0.0386(0.1205)$ $\{R_1 = \sum||F_o| - |F_c|| / \sum|F_o|$; $wR_2 = \sum[w(F_o^2 - F_c^2)^2] / \sum[w(F_o^2)^2]^{1/2}\}$. A summary of crystal data and structure refinement for **1** is provided in Table 1. The selected bond lengths and band angles are listed in Table 2. The atomic coordinates and equivalent isotropic displacement parameters for **1** are given in Table 3. Crystallographic data (excluding structure factors) for the structure reported in this paper have been deposited with the Cambridge Crystallographic Data Centre as supplementary publication No. CCDC 228759.

Table 1
Crystal data and structure refinement for **1**

Empirical formula	$C_9H_{23}BaMo_4N_3O_{17}$
Formula weight	966.40
Temperature	293(2) K
Wavelength	0.71073 Å
Crystal system	Triclinic
Space group	$P\bar{1}$
Unit cell dimensions	$a = 9.984(2)$ Å; $\alpha = 115.86(3)°$ $b = 11.117(2)$ Å; $\beta = 97.66(3)°$ $c = 12.681(3)$ Å; $\gamma = 98.11(3)°$
Volume	1223.5(4) Å^3
Z	2
D_{cal}	2.623 mg/m^3
Absorption coefficient	3.658 mm^{-1}
θ range for data collection	2.04–27.47°
Reflections collected	8833
Independent reflections	5535 [$R_{(int)} = 0.0424$]
Data/restraints/parameters	5535/0/308
Final R indices [$I > 2\sigma(I)$]	$R_1 = 0.0386$, w$R_2 = 0.1205$
R indices (all data)	$R_1 = 0.0399$, w$R_2 = 0.1226$

3. Results and discussion

3.1. Description of the structure

The single-crystal X-ray diffraction analysis reveals that compound **1** exhibits a novel 2D framework built from octamolybdate supported units. As shown in Fig. 1, the $\{Mo_8O_{26}\}^{4-}$ moiety consists of eight edge-sharing $\{MoO_6\}$ octahedra and displays the characteristic β-octamolybdate arrangement, a classical isomer of octamolybdate clusters, in which two centrosymmetrically related cyclic $\{Mo_4O_{13}\}$ units are cross-linked by

Table 2
Selected bond lengths (Å) and angles (deg) for **1**

Ba(1)–O(15)	2.694(3)	Ba(1)–O(2)	2.898(3)
Ba(1)–O(14)#1	2.739(3)	Ba(1)–O(14)	2.900(3)
Ba(1)–O(1)	2.777(3)	Ba(1)–O(7)#2	2.951(3)
Ba(1)–O(1W)	2.840(5)	Ba(1)–O(3)	3.015(3)
Ba(1)–O(5)	2.878(3)	Ba(1)–O(1W)#1	3.315(8)
Mo(1)–O(9)	1.694(3)	Mo(2)–O(7)	1.702(2)
Mo(1)–O(1)	1.724(3)	Mo(2)–O(2)	1.708(3)
Mo(1)–O(6)	1.917(2)	Mo(2)–O(12)	1.884(3)
Mo(1)–O(12)	1.928(3)	Mo(2)–O(10)	2.014(2)
Mo(1)–O(8)#3	2.268(3)	Mo(2)–O(11)#3	2.291(3)
Mo(1)–O(13)	2.427(2)	Mo(2)–O(13)	2.342(2)
Mo(3)–O(3)	1.697(3)	Mo(4)–O(4)	1.701(3)
Mo(3)–O(8)	1.750(2)	Mo(4)–O(5)	1.711(3)
Mo(3)–O(11)	1.946(2)	Mo(4)–O(6)	1.898(3)
Mo(3)–O(10)	1.950(2)	Mo(4)–O(11)	2.006(2)
Mo(3)–O(13)	2.147(2)	Mo(4)–O(10)#3	2.294(3)
Mo(3)–O(13)#3	2.314(3)	Mo(4)–O(13)	2.337(2)
O(1)–Mo(1)–O(13)	91.69(11)	O(7)–Mo(2)–O(2)	106.10(13)
O(6)–Mo(1)–O(13)	74.84(9)	O(7)–Mo(2)–O(12)	101.75(13)
O(12)–Mo(1)–O(13)	74.09(9)	O(2)–Mo(2)–O(12)	101.58(13)
O(8)#3–Mo(1)–O(13)	70.13(9)	O(7)–Mo(2)–O(10)	102.14(12)
O(9)–Mo(1)–O(1)	105.94(15)	O(2)–Mo(2)–O(10)	95.26(12)
O(9)–Mo(1)–O(6)	103.34(13)	O(12)–Mo(2)–O(10)	145.51(10)
O(3)–Mo(3)–O(8)	106.27(13)	O(4)–Mo(4)–O(5)	106.05(14)
O(3)–Mo(3)–O(11)	101.18(12)	O(4)–Mo(4)–O(6)	102.38(13)
O(8)–Mo(3)–O(11)	96.46(11)	O(5)–Mo(4)–O(6)	101.10(13)
O(3)–Mo(3)–O(10)	100.95(12)	O(4)–Mo(4)–O(11)	100.62(12)
O(8)–Mo(3)–O(10)	96.35(11)	O(5)–Mo(4)–O(11)	95.45(12)
O(11)–Mo(3)–O(10)	150.11(10)	O(6)–Mo(4)–O(11)	146.56(10)
O(15)–Ba(1)–O(14)#1	69.90(11)	O(1)–Ba(1)–O(1W)	126.61(11)
O(15)–Ba(1)–O(1)	144.78(10)	O(15)–Ba(1)–O(5)	123.45(10)
O(14)#1–Ba(1)–O(1)	132.37(9)	O(14)#1–Ba(1)–O(5)	131.86(9)
O(15)–Ba(1)–O(1W)	86.40(14)	O(1)–Ba(1)–O(5)	66.36(9)
O(14)#1–Ba(1)–O(1W)	62.71(15)	O(1W)–Ba(1)–O(5)	71.79(13)
O(1)–Ba(1)–O(2)	64.48(8)	O(5)–Ba(1)–O(2)	93.16(8)
O(1W)–Ba(1)–O(2)	150.14(17)	O(15)–Ba(1)–O(14)	143.76(11)

Symmetry transformations used to generate equivalent atoms: #1$-x+1$, $-y+1$, $-z$; #2$-x+1$, $-y$, $-z$; #3$-x$, $-y$, $-z$.

Table 3
Atomic coordinates ($\times 10^4$) and equivalent isotropic displacement parameters ($A^2 \times 10^3$) for **1**

	x	Y	z	U_{eq}
Ba(1)	4321(1)	3428(1)	472(1)	25(1)
Mo(1)	1631(1)	−151(1)	−2409(1)	21(1)
Mo(2)	2652(1)	−710(1)	−149(1)	20(1)
Mo(3)	907(1)	1419(1)	1368(1)	17(1)
Mo(4)	−111(1)	1987(1)	−854(1)	20(1)
O(1)	3048(3)	1212(3)	−1747(2)	28(1)
O(2)	3900(3)	766(3)	416(3)	26(1)
O(3)	2330(3)	2697(3)	1802(2)	27(1)
O(4)	−1340(3)	2749(3)	−1201(3)	32(1)
O(5)	1398(3)	3219(3)	−212(3)	27(1)
O(6)	226(3)	866(3)	−2380(2)	24(1)
O(7)	3460(3)	−1894(3)	0(3)	28(1)
O(8)	292(3)	1692(3)	2666(2)	25(1)
O(9)	1670(3)	−969(3)	−3883(2)	34(1)
O(10)	1762(2)	−85(2)	1279(2)	19(1)
O(11)	−491(3)	2101(2)	697(2)	20(1)
O(12)	2387(3)	−1297(3)	−1813(2)	26(1)
O(13)	977(2)	429(2)	−498(2)	18(1)
O(14)	3427(3)	4462(4)	−1182(3)	40(1)
O(15)	5644(4)	4181(4)	2733(3)	48(1)
O(16)	5146(7)	7985(6)	3692(4)	91(2)
N(1)	7031(4)	4802(4)	4517(3)	41(1)
N(2)	1452(4)	3789(4)	−2585(3)	35(1)
N(3)	5765(5)	9120(5)	5704(4)	49(1)
C(1)	5280(7)	9262(9)	6766(6)	73(2)
C(2)	7149(6)	9776(7)	5848(5)	53(1)
C(3)	4920(8)	8273(7)	4628(6)	67(2)
C(4)	574(6)	2755(6)	−3731(4)	51(1)
C(5)	901(6)	4969(6)	−1902(6)	55(1)
C(6)	2659(5)	3638(4)	−2172(4)	34(1)
C(7)	6601(7)	6079(6)	5136(5)	57(1)
C(8)	8069(8)	4499(8)	5222(7)	78(2)
C(9)	6503(5)	3972(5)	3360(4)	41(1)
O(1W)	3846(6)	6122(6)	1375(5)	95(2)

bridging oxygen atoms. All molybdenum sites exhibit +VI oxidation state, possessing octahedral coordination geometry with different distortion extents. The +VI oxidation state is also confirmed by bond valence sum calculations [20], which give the values of 5.959(45), 5.928(41), 5.938(38), and 5.902(41) for Mo(1), Mo(2), Mo(3), and Mo(4). The average value for the calculated oxidation states of Mo is 5.932(41), showing that all Mo sites are in the +6 oxidation state. The result is consistent with the formula of the title compound given by X-ray structure determination. The Mo–O bonds can be divided into four groups, i.e. Mo–O(t) bonds, Mo–O(μ_2) bonds, Mo–O(μ_3) bonds, and Mo–O(μ_5) bonds, whose bond distances fall in the ranges 1.649(3)–1.724(3), 1.750(2)–2.268(3), 1.946(2)–2.294(3), and 2.147(2)–2.427(2) Å, and the mean values are 1.705, 1.943, 2.097, and 2.313 Å, respectively. These results shows that MoO_6 octahedra of anion are severely distorted, indicating that the strong interaction between the polyanions and $[Ba(DMF)_2(H_2O)]_2^{4+}$ units. In each decanuclear $[Ba(DMF)_2(H_2O)]_2[Mo_8O_{26}]$, two crystallographically identical Ba^{2+} ions, Ba1 and Ba1A, are located at opposite sites of the polyanion, thus forming a sandwich-like structure. The coordination environment around Ba^{2+} ion is depicted in Fig. 2. Each Ba^{2+} ion is surrounded by 10 oxygen atoms, in which three oxygen atoms (Ba(1)–O(14) = 2.900(3) Å, Ba(1)–O(14A) = 2.739(3) Å, Ba(1)–O(15) = 2.694(3) Å) from DMF molecules, two oxygen atoms (Ba(1)–O(1W) = 2.840(5) Å, Ba(1)–O(1WA) = 3.315(8) Å) from aqua ligands, four oxygen atoms (Ba(1)–O(1) = 2.777(3) Å, Ba(1)–O(2) = 2.898(3) Å, Ba(1)–O(3) = 3.015(3) Å, Ba(1)–O(5) = 2.878(3) Å) from one octamolybdate cluster, and the remaining one (Ba(1)–O(7) = 2.951(3) Å) from the other octamolybdate cluster. It should be noteworthy that the connection between barium ions in **1** relies on four bridging oxygen atoms, two from aqua ligands, and two from DMF molecules,

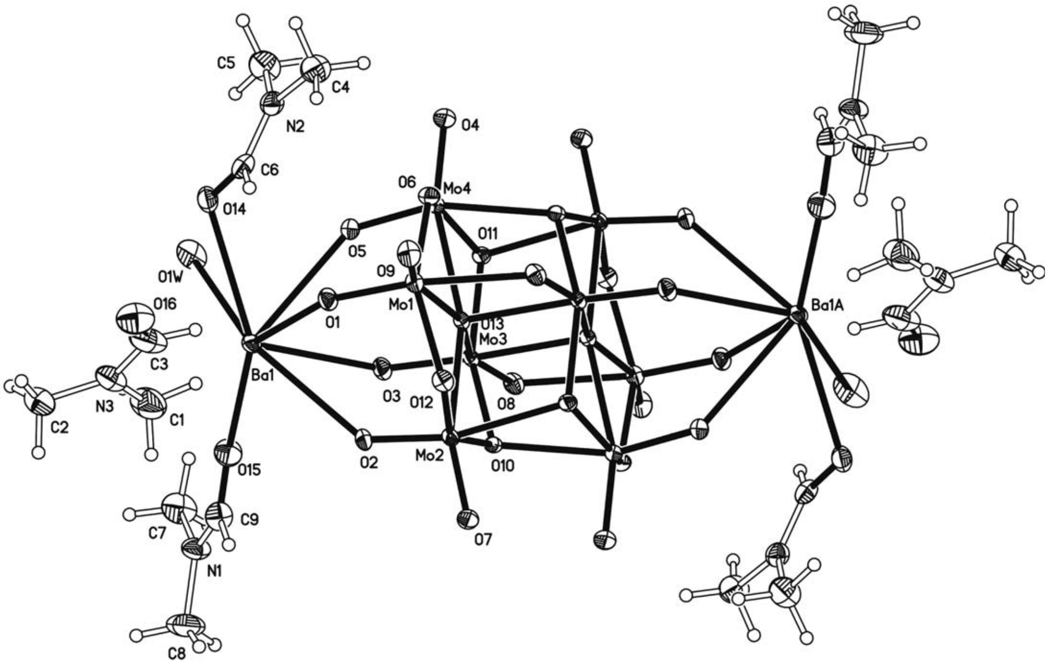

Fig. 1. Molecular structure unit of compound **1**.

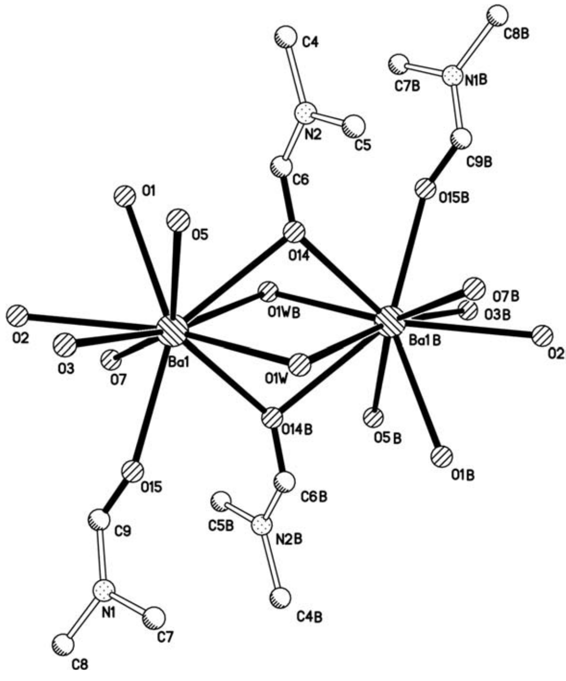

Fig. 2. Coordination environment of Ba^{2+}in **1**.

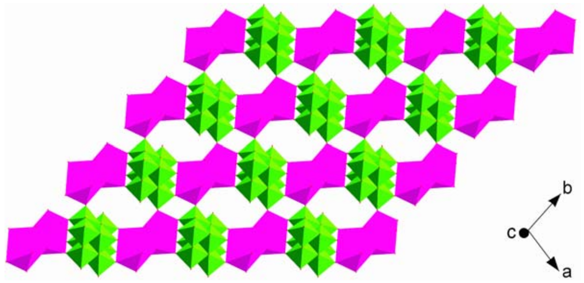

Fig. 3. A polyhedral representation of the 2D layered in **1**. DMF molecules are omitted for clarity.

which is similar to that of a 1D Keggin-typed polyanion supported compound [21]. The non-bonding Ba···Ba distance is 4.2703 Å.

In fact, the two-dimensional structure of **1** can be best described as follows: first, the adjacent β-octamolybdate bi-supported building blocks $[Ba(DMF)_2(H_2O)]_2[Mo_8O_{26}]$ are interconnected via Ba–O–Ba bridges, forming an infinite chain, and then the adjacent chains are further linked via Mo–O–Ba bridges constructing a 2D layer running along the [001] direction (Fig. 3). As we can see from Fig. 3, each β-$[Mo_8O_{26}]^{4-}$ ion furnishes 10 oxygen atoms (O1, O1A, O2, O2A, O3, O3A, O5, O5A, O7, O7A) to take part in coordination. It should be noted that the 10 oxygen atoms play different roles in the construction of the 2D sheet. Four oxygen atoms of a β-$[Mo_8O_{26}]^{4-}$ cluster, i.e. O1, O2, O3, O5, connected with one Ba^{2+} ion in one side, another four symmetrically related oxygen atoms (O1A, O2A, O3A, O5A) connect with the other crystallographically identical Ba^{2+} ion in the opposite direction, forming a $[Ba(DMF)_2(H_2O)]_2[Mo_8O_{26}]$ unit. All such units are linked together in virtue of Ba–O–Ba linkage to give a 1D chain. That is to say the above eight oxygen atoms are mainly used to form 1D chain. Whereas the remaining two oxygen atoms (O7 and O7A) connect

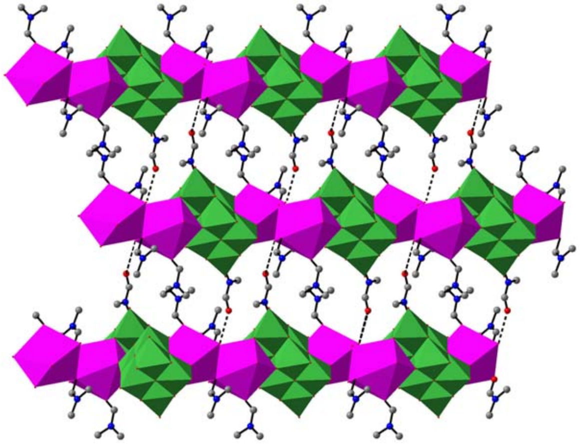

Fig. 4. View of the stacking arrangement of **1**, showing hydrogen-bonding interactions.

with Ba^{2+} ions of adjacent chains, thereby extending these chains into a 2D layer. This phenomenon in which each polyanion offers 10 coordination sites is still rare in the reported complexes participated by polyanion cluster. Neighboring sheets are further extended into 3D supramolecular network through hydrogen-bonding interactions (Fig. 4). Isolated DMF molecules are distributed between layers and form strong hydrogen bonds with coordinated water molecules from 2D layer. The representative hydrogen bond is O1W⋯O16, whose length is 2.743 Å. Interestingly, the adjacent 2D layers are parallel and stacked without interpenetration to generate 1D parallelogram channels along the c−axis, with pores open of 9.1×4.5 Å established by the O⋯O distance (9.1 Å) and the nearest Ba⋯Mo distance (4.5 Å), respectively.

3.2. IR spectroscopy

In the IR spectrum of the title compound, the characteristic bonds at 938, 912, 837, 732, 694, and 665 cm^{-1} are attributed to the Mo=O and Mo–O–Mo vibrations. Comparing the IR spectrum of compound **1** with that of β-$[Mo_8O_{26}]^{4-}$ [22], it can be observed that the shape of the peaks in the range 600–1000 cm^{-1} is nearly identical to that of β-$[Mo_8O_{26}]^{4-}$ except slight shifts of some peaks due to the effect of coordination, which indicates that the polyanion in the title compound still retains the basic β-$[Mo_8O_{26}]^{4-}$ structure. This is in agreement with the result of single-crystal X-ray diffraction analysis. In addition, the resonances at 1654 and 1106 cm^{-1} in compound **1** are assigned to the ν_{as} (C=O) and ν_{as} (C–N) asymmetric stretching vibrations of DMF molecule. The IR spectrum studies indicate that there is strong interaction between the polyanions and organic groups in solid state.

3.3. TG analyses

Thermogravimetric analysis of compound **1** shows four continuous weight loss steps. The first step (7.45%) in the temperature ca. 85–145°C corresponds to the loss of two-isolated DMF molecules (7.56%). The second step (7.51%) in the temperature range ca. 145–220°C corresponds to the loss of two-coordinated DMF molecules. The third step (7.49%) occurs in the temperature range 220–335°C, corresponding to the removal of the other two-coordinated DMF molecule. The fact that the two-coordinated DMF molecules bonding to the same barium site disassociated at different temperature perhaps results from the strength difference of the interaction between DMF molecule and the β-$[Mo_8O_{26}]^{4-}$ moiety. The fourth step weight loss started at ca. 335°C up to 380°C to give a weight loss of ca. 2.07%, corresponding to the loss of two-coordinated water molecules (1.86%). The remaining weight of 75.48% indicates that the final product is MoO_3 and BaO (75.44%). It can be observed that the result of the TG analysis basically agrees with that of the structure determination.

3.4. Electrochemical property

3.4.1. Apparatus

A CHI 660 Electrochemical Workstation connected to a Digital-586 personal computer was used for control of the electrochemical measurements and for data collection. A conventional three-electrode cell, consisting a 1-based modified carbon paste electrode (POM**1**-CEP) or a bare CEP as the working electrode, a saturated calomel reference electrode (SCE) and a Pt gauze counter electrode was used. All potentials were measured and reported versus the SCE. All the experiments were conducted at room temperatures (20–25°C).

3.4.2. Fabrication of the POM**1**-CEP and the base CPE

The POM**1**-CEP was fabricated as follows: 1.0 g graphite powder was added to the solution of 2 mL acetone containing 30 mg **1** and the mixture was ultrasonically mixed for 3 min, followed by evaporation of acetone, which produced rather homogenously covered graphite particles. To the graphite particles 0.66 mL Nujol was added and stirred with a glass stick. The homogenized mixture was used to pack 3 mm inner diameter glass tube to a length of 0.8 cm from one of its ends. In addition, a little extra mixture was retained on the top of the electrodes, and the mixture in the tube was pressed lightly on smooth plastic paper with a copper stick through the back. The electrical contact was established with the copper stick. The bare CEP was fabricated using the same procedure as described above

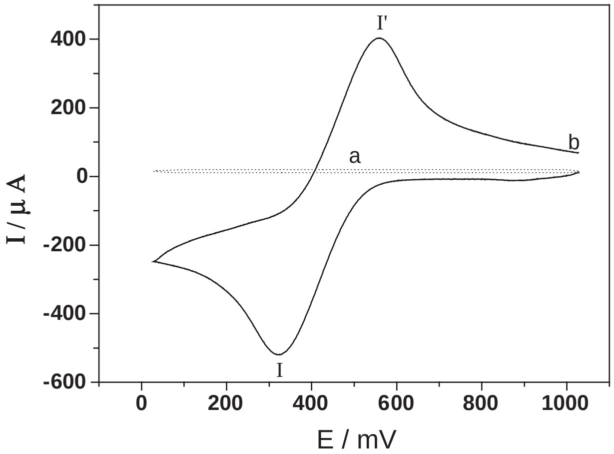

Fig. 5. Cyclic voltammograms of (a) the bare CEP and (b) the POM**1**-CEP in 1 M H_2SO_4 at a scan rate of $100\,mV\,s^{-1}$.

except that the modifier in acetone was not added. The surface of the CEP was wiped with weighing paper.

3.4.3. *Electrochemical behavior of the POM1-CEP*

The electrochemical studies of the POM**1**-CEP were carried out in 1 M H_2SO_4 aqueous solution. Fig. 5 shows the cyclic voltammograms in 1 M H_2SO_4 aqueous solution at a bare CPE and POM**1**-CEP. It can be seen from Fig. 5 that in the potential range + 1000–0 mV (versus SCE), there is no redox peak at the bare CEP, while at the POM**1**-CEP, one reversible redox peak appears. The mean peak potential $E_{1/2} = (E_{pa} + E_{pc})/2$ is + 413 mV (I). The redox peak $I - I'$ might be ascribed to Mo^{VI}/Mo^{V}. Furthermore, the POM**1**-CEP possesses high stability. When the potential range is maintained at + 1000 to 0 mV, the peak currents almost keep unchanged over 300 cycles at a rate of $100\,mV\,s^{-1}$. Compared with POMs-modified film electrodes fabricated by conventional methods, the POM**1**-CEP has certain advantages: it is inexpensive, easy to handle, easy to prepare, and above all, the electrode surface can be renewed after every use. A fresh surface can be exposed by means of squeezing a little carbon paste out of tube whenever needed. This is especially useful for electrocatalytic study since the catalytic activity is known to decrease when the electrode is fouled.

4. Conclusions

In conclusion, a novel 2D β-octamolybdate supported alkaline-earth metal complex, $[Ba(DMF)_2(H_2O)]_2[Mo_8O_{26}] \cdot 2DMF$, has been synthesized by the direct modification to the surface of polyanion cluster and characterized by single-crystal X-ray diffraction, IR spectrum and TG analysis. The synthesis of the compound not only contributes to acquiring some information on the optical properties of such kinds of complexes but also offers a valuable clue to the preparation of other isopolyoxomolybdate (such as Lindqvist structure) supported organic–inorganic hybrid complexes.

Acknowledgments

This work is financially supported by the National Natural Science Foundation of China (Grant 20171010).

References

[1] E. Coronado, C.J. Gomez-Garcia, Chem. Rev. 98 (1998) 273–296.
[2] D. Hagrman, R.C. Haushalter, J. Zubieta, Chem. Mater. 10 (1998) 361–365.
[3] C.L. Hill (Guest Ed.), Chem. Rev. 98 (1998) 1–389.
[4] D.W. Brrace, D. O'Hare (Eds.), Inorganic Materials, Wiley, Chichester, 1992.
[5] M.C. Petty, M.R. Bryce, D. Bloor (Eds.), Introduction to Molecular Electronics, Edward Arnold, London, 1995.
[6] N. Masciocchi, D. Cairati, L. Carlucci, G. Mezza, G. Ciani, A. Sireni, J. Chem. Soc. Dalton Trans. (1996) 2739–2746.
[7] M.T. Pope, A. Müller, Angew. Chem. Int. Ed. 30 (1991) 34–48.
[8] M.T. Pope, Heteropoly and Isopoly Oxometalates, Springer, New York, 1983.
[9] (a) Y.G. Li, E.B. Wang, H. Zhang, G.Y. Luan, C.W. Hu, J. Solid State Chem. 163 (2002) 10–16;
(b) S.T. Wang, Y.G. Li, E.B. Wang, C.W. Hu, N.H. Hu, H.Q. Jia, J. Solid State Chem. 167 (2002) 402–406;
(c) L. Xu, Y. Sun, E.B. Wang, E. Shen, Z. Liu, C.W. Hu, Y. Xing, Y. Lin, H.Q. Jia, New J. Chem. 23 (1999) 1041–1044;
(d) C. Qin, L. Xu, Y.G. Wei, X.L. Wang, F.Y. Li, Inorg. Chem. 42 (2003) 3107–3110;
(e) L. Xu, C. Qin, X.L. Wang, Y.G. Wei, E.B. Wang, Inorg. Chem. 42 (2003) 7342–7344;
(f) Y. Lu, E.B. Wang, M. Yuan, G.Y. Luan, Y.G. Li, J. Chem. Soc. Dalton Trans. (2002) 3029–3031;
(g) Y.G. Li, G.J.H. De, M. Yuan, E.B. Wang, R.D. Huang, C.W. Hu, N.H. Hu, H.Q. Jia, J. Chem. Soc. Dalton Trans. (2003) 331–334;
(h) Y.M. Chen, E.B. Wang, B.Z. Lin, S.T. Wang, J. Chem. Soc. Dalton Trans. (2003) 519–520;
(i) G.Y. Luan, Y.G. Li, S.T. Wang, E.B. Wang, Z.B. Han, C.W. Hu, N.H. Hu, H.Q. Jia, J. Chem. Soc. Dalton Trans. (2003) 233–235.
[10] B. Yan, Y. Xu, X. Bu, N.K. Goh, L.S. Chia, G.D. Stucky, J. Chem. Soc. Dalton Trans. (2001) 2009–2014.
[11] Y.H. Wang, L.D. Chen, C.W. Hu, E.B. Wang, H.Q. Jia, N.H. Hu, J. Solid State Chem. 161 (2001) 173–176.
[12] J.H. Wang, R.Z. Wang, G.Y. Yang, Y.H. Xing, D.M. Li, W.M. Bu, L. Ye, Y.G. Fan, G.D. Yang, Y. Xing, Y.H. Lin, H.Q. Jia, Chem. Commun. (1999) 983–984.
[13] P.J. Zapf, C.J. Warren, R.C. Haushalter, J. Zubieta, Chem. Commun. (1997) 1543–1544.
[14] J.R.D. DeBord, R.C. Haushalter, L.M. Meyer, J. Zubieta, Inorg. Chem. 36 (1997) 2159–2165.
[15] D. Hagrman, C. Zubieta, D.J. Rose, J. Zubieta, R.C. Haushalter, Angew. Chem. Int. Ed. 36 (1997) 795.
[16] D. Hagrman, C. Sangregorio, C.J. O'Connor, J. Zubieta, Chem. Commun. (1998) 1283–1284.

[17] C.D. Wu, C.Z. Lu, X. Lin, H.H. Zhuang, J.S. Huang, Inorg. Chem. Commun. 5 (2002) 664–666.

[18] M. Filowitz, R.K.C. Ho, W.G. Klemperer, W. Shum, Inorg. Chem. 18 (1979) 93–103.

[19] (a) G.M. Sheldrick, SHELXL97, Program for Crystal Structure Refinement; University of Göttingen, Göttingen, Germany, 1997;
(b) G.M. Sheldrick, SHELXL97, Program for Crystal Structure Solution, University of Göttingen, Göttingen, Germany, 1997.

[20] D. Brown, D. Altermatt, Acta Crystallogr. B 41 (1985) 244–247.

[21] J.Y. Niu, Q. Wu, J.P. Wang, J. Chem. Soc. Dalton Trans. (2002) 2512–2516.

[22] W.G. Klemperer, W. Shum, J. Am. Chem. Soc. 98 (1976) 8291–8293.